STRUCTURAL PERFORMANCE OF PRECAST PRESTRESSED CONCRETE FRAMES WITH HYBRID POST-TENSIONED CONNECTIONS

Takeaki KOSHIKAWA[1], Masaiki UEDA[2], Masaru KIKUCHI[3] and Takasuke SAITO[4]

[1] *Assistant Professor, Graduate School of Engineering, Hokkaido University, Sapporo, Japan*
[2] *Professor, Graduate School of Engineering, Hokkaido University, Sapporo, Japan*
[3] *Associate Professor, Graduate School of Engineering, Hokkaido University, Sapporo, Japan*
[4] *Graduate Student, Graduate School of Engineering, Hokkaido University, Sapporo, Japan*
Email: takeaki@eng.hokudai.ac.jp

ABSTRACT:

This paper discusses the structural performance of precast prestressed concrete frames connected by hybrid post-tensioned connections under cyclic loading. The discussion is based on an analysis performed using analytical models comprised of a prestressed concrete frame element with a bond slip in the unbonded prestressing tendon, and a beam-column joint element with a bond slip. The accuracy of the analytical models is illustrated by comparing the behavior of the models with the results of previous experiments conducted on beam-to-column subassemblies with hybrid post-tensioned connections. Following this, an analytical parametric study is presented that investigates the effects of variations in the connection details on the behavior of the subassemblies. The results of this study indicate that the energy dissipation of these subassemblies can be estimated from the amount of bonded reinforcing steel bars, and that the self-centering capability can be evaluated from the ratio of the level of initial prestressing force to the amount of bonded reinforcing steel bars.

KEYWORDS: Precast prestressed Concrete Frame, Hybrid Post-Tensioned Connection, Hysteretic Behavior, Bond Slip, Material Nonlinear Analysis

1. INTRODUCTION

Precast prestressed concrete frames connected by unbonded prestressing tendons combine the potential benefits of construction speed and high quality control. Although this type of frame has high restoring-force characteristics under cyclic loading, the energy dissipation capability of the frame is relatively low. In order to enhance the energy dissipation capability of precast prestressed concrete frames, while retaining their small residual deformation characteristics, a new precast framing system connected by hybrid post-tensioned connections has been developed [1, 2].

The precast framing system uses the gap-opening behavior at the beam-to-column interface to provide energy dissipation without transmitting damaging force to the main structural members. The hybrid post-tensioned connection uses both unbonded prestressing tendon and bonded reinforcing steel bar. In this connection, the unbonded prestressing tendon is specifically designed not to yield, because its function is to maintain the clamping force between the beam and the column, and to provide a reliable and permanent self-centering restoring force. The bonded reinforcing steel bars are intentionally designed to yield in order to dissipate energy under cyclic loading.

This paper analytically investigates the structural performance of precast prestressed concrete frames connected by hybrid post-tensioned connections under cyclic loading and provides described analytical models. The models are verified by comparing the results of experimental study. After which, an analytical parametric study is presented that investigates the effects of variations in the connection details on the behavior of the frames.

2. OUTLINE OF ANALYTICAL MODELS

For the purpose of analyzing the performance of the precast prestressed concrete frames connected by hybrid post-tensioned connections, two numerical models based on the finite element method were used in this paper. One is a frame element [3], and the other is a beam-column joint element [4]. These elements include the bond slip effects between reinforcing steel bars and concrete, and between bonded or unbonded prestressing tendons and concrete. They can be applied to the response analysis of both reinforced concrete frame structures and prestressed concrete frame structures by using the appropriate constitutive laws for each structure.

2.1. Frame Element with Bond Slip

The frame element with bond slip is shown in Figure 1 [3]. The element has two nodes with three + m degrees of freedom per node. The concrete cross-section of the element is composed of a discrete number of concrete layers, and steel layers for both reinforcing steel bars and prestressing tendons are incorporated in some of the concrete layers. Each steel layer has a bond interface. The element formulation in the incremental form, based on the principle of minimum potential energy, is briefly described hereafter.

The displacement field for the frame element with a bond slip consists of displacements u, w, s_1, …, s_i, …, s_m, where u and w are the axial and vertical displacements, respectively, at the reference axis x, and s_i is the slip displacement of steel layer i. The slip displacement is the relative displacement between the concrete and the steel layer. Using the displacement field notation, the section displacement increment Δu_{ci} of a concrete layer i at distance z_i from the reference axis x, and the section displacement increment Δu_{si} of a steel layer i at distance z_{si} from the reference axis x are given by,

$$\Delta u_{ci} = \Delta u - z_i \frac{d\Delta w}{dx} \tag{2.1}$$

$$\Delta u_{si} = \Delta u - z_{si} \frac{d\Delta w}{dx} + \Delta s_i \tag{2.2}$$

Strain and stress increments at these layers based on the Euler-Bernoulli beam theory are given by,

$$\Delta \varepsilon_{ci} = \frac{d\Delta u}{dx} - z_i \frac{d^2\Delta w}{dx^2} \tag{2.3}$$

$$\Delta \varepsilon_{si} = \frac{d\Delta u}{dx} - z_{si} \frac{d^2\Delta w}{dx^2} + \frac{d\Delta s_i}{dx} \tag{2.4}$$

$$\Delta \sigma_{ci} = E_{ci} \Delta \varepsilon_{ci} \tag{2.5}$$

$$\Delta \sigma_{si} = E_{si} \Delta \varepsilon_{si} \tag{2.6}$$

where ε_{ci} and ε_{si} are the strain of concrete and steel layer i, σ_{ci} and σ_{si} are the stress of concrete and steel layer i, and E_{ci} and E_{si} are the stiffness of concrete and steel layer i, respectively. The relationship between slip displacement s_i and bond stress τ_{bi} at the bond interface of steel layer i is assumed in the following equation.

$$\Delta \tau_{bi} = K_{bi} \Delta s_i \tag{2.7}$$

where K_{bi} is the bond stiffness of steel layer i.

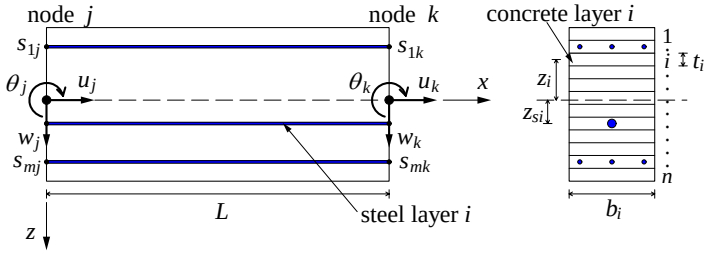

Figure 1 Frame element with bond slip

The equilibrium equations along with the boundary and continuity conditions are derived using the principle of minimum potential energy, which requires that

$$\delta\Delta\Pi = \delta(\Delta U - \Delta V) = 0 \tag{2.8}$$

where Π is the total potential energy functional, U is the strain energy, V is the potential of the external loads, and δ is the variational operator. The strain energy U for the frame element under consideration can be written

$$\Delta U = \Delta U_c + \Delta U_s + \Delta U_b \tag{2.9}$$

where U_c and U_s are the strain energies in the concrete and steel, respectively, and U_b is the potential energy of the bond slip. Using the relation of Eqns. 2.3 – 2.7, these energies are given by

$$\Delta U_c = \frac{1}{2}\int_0^L \left(\sum_{i=1}^{n} b_i t_i \Delta\sigma_{ci}\Delta\varepsilon_{ci} - \sum_{i=1}^{m} A_{si}\Delta\sigma_{ci}\Delta\varepsilon_{ci} \right) dx \tag{2.10}$$

$$\Delta U_s = \frac{1}{2}\int_0^L \left(\sum_{i=1}^{m} A_{si}\Delta\sigma_{si}\Delta\varepsilon_{si} \right) dx \tag{2.11}$$

$$\Delta U_b = \frac{1}{2}\int_0^L \left(\sum_{i=1}^{m} A_{bi}\Delta\tau_{bi}\Delta s_i \right) dx \tag{2.12}$$

where L is the element length, n is number of concrete layers, b_i and t_i are the width and thickness of the concrete layer i, respectively, m is number of steel layers, A_{si} is the sectional area of the steel layer i, and A_{bi} is the bond area per unit length of the steel layer i.

In the finite element formulation based on the displacement method, the element displacements are expressed as functions of the nodal displacement through the displacement shape functions. A linear shape function for the axial displacement, a cubic shape function for the vertical displacement, and a linear shape function for the slip displacement are used. Substituting Eqns. 2.3 – 2.7, 2.9 – 2.12 into Eqn. 2.8, and using these element displacements, the finite element equation for the frame element with bond slip is derived as follows:

$$\begin{bmatrix} \mathbf{K}_{uu} & \mathbf{K}_{uw} & \mathbf{K}_{us} \\ & \mathbf{K}_{ww} & \mathbf{K}_{ws} \\ sym. & & \mathbf{K}_{ss} \end{bmatrix} \begin{Bmatrix} \Delta\mathbf{u} \\ \Delta\mathbf{w} \\ \Delta\mathbf{s} \end{Bmatrix} = \begin{Bmatrix} \Delta\mathbf{P}_u \\ \Delta\mathbf{P}_w \\ \Delta\mathbf{P}_s \end{Bmatrix} \tag{2.13}$$

where $\mathbf{K}_{uu}$, $\mathbf{K}_{uw}$, $\mathbf{K}_{us}$, $\mathbf{K}_{ww}$, $\mathbf{K}_{ws}$ and $\mathbf{K}_{ss}$ are the terms in the element stiffness matrix, $\mathbf{u}$ and $\mathbf{w}$ are the nodal displacement vectors for the axial and vertical displacement, $\mathbf{s}$ is the slip displacement vector at the nodes with respect to all steel layers, and $\mathbf{P}_u$, $\mathbf{P}_w$ and $\mathbf{P}_s$ are the nodal force vectors corresponding to the displacement vectors $\mathbf{u}$, $\mathbf{w}$ and $\mathbf{s}$, respectively. The finite element equation, in which the slip displacement s_i is incorporated as the nodal displacement, makes it possible to estimate the influence of the bond slip of steel bars directly by following the general solution for the finite element equation, without the need to take any special calculation steps.

The constitutive components of the frame element are the concrete layers, the steel layers, and bond interfaces. Material nonlinearity for each component is expressed by uniaxial cyclic constitutive laws. These laws are illustrated in Figure 2. In compression, the monotonic stress-strain relation of concrete is represented by the Saenz' equation [5] in the ascending range and a linear relation for the descending post peak part until reaching the point where the stress becomes zero. When analyzing concrete members exhibiting a compression softening response, element size dependence due to the strain localization occurs. To resolve this dependence, compressive fracture energy is introduced into the gray-shaded section in the figure. The value for compressive fracture energy G_{fc} is determined using the equation proposed by Nakamura and Higai [6]. Under tension, the linear elastic behavior is assumed up to the cracking point, with tension softening characteristics for increasing tensile strains. For tension softening characteristics, the 1/4 model, which reduces stress in two steps, is used. In response to cyclic loading, a linear branch is assumed on the tensile side between the starting point of unloading and the original point. On the compressive side, a linear branch that connects the starting point of unloading and residual strain point is assumed. In this case, the value of the residual strain is established in accordance with

the value of the unloading starting point strain using the experimental formula proposed by Karsan and Jirsa [7]. For steel, the bilinear model is used for the monotonic stress-strain relations, and the Menegotto-Pinto model is used for the hysteretic stress-strain relations. The bond stress-slip relation between bonded steel bar and concrete is multiple lines for the monotonic envelope, and the model of Ueda and Dobashi [8], which is modified from the model of Morita and Kaku [9], for the hysteretic behavior. For unbonded tendon, a linear elastic bond stress-strain relation with relatively low bond stiffness is assumed.

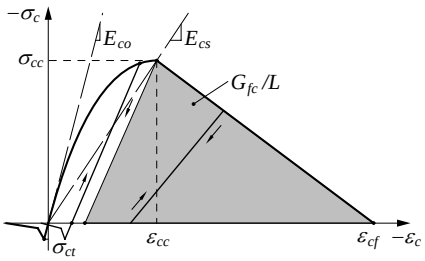

Stress-strain relation of concrete

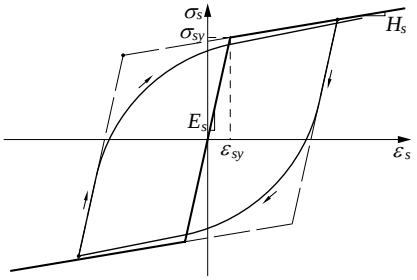

Stress-strain relation of steel

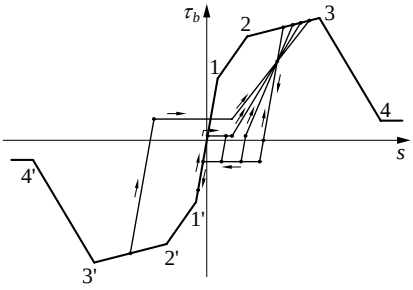

Bond stress-slip relation of bonded steel bar

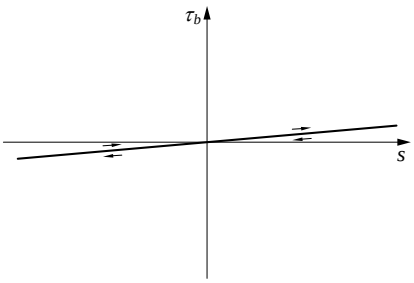

Bond stress-slip relation of unbonded tendon

Figure 2 Uniaxial constitutive laws

2.2. Beam-Column Joint Element with Bond Slip

The beam-column joint element with bond slip is shown in Figure 3 [4]. The joint element is composed of two frame elements with bond slips that are perpendicular to each other. The element has four nodes, and the axial displacements, vertical displacements, and rotations at each node are linked to represent the rigid body mode response of the joint element. The slip displacements are independent of the linked displacements, thus the continuity of slip displacement of the steel bars or tendons between the frame element and the joint element is maintained.

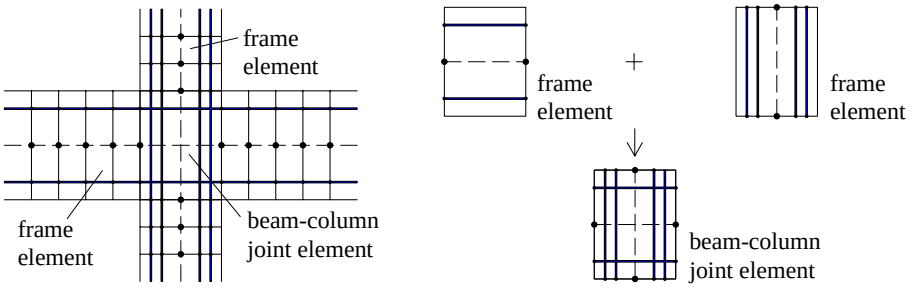

Figure 3 Beam-column joint element with bond slip

3. COMPARISON WITH EXPERIMENTAL RESULTS

Stone et al. [1] tested a series of beam-to-column subassemblies with a hybrid post-tensioned connection. Two

of these subassemblies, specimens M-P-Z4 and O-P-Z4, were selected for study in order to verify the accuracy of the models. The configuration of these specimens is the same and is shown in Figure 4. The specimens are constructed by post-tensioning precast beams onto precast columns using unbonded prestressing strands, and by grouting reinforcing steel bars arranged at the top and bottom of the beam. The reinforcing steel bars are passed through the beam-column connection. The basic rationale behind the arrangements for these specimens is to use the bonded (grouted) reinforcing steel bars as energy dissipators while using the unbonded prestressing strands to maintain the clamping force between the beam and column, and to provide a reliable and permanent self-centering restoring force. In these specimens, only the amount of the bonded reinforcing steel bars is different. Specimen M-P-Z4 had two No. 3 (top and bottom) bonded reinforcing steel bars; while specimen O-P-Z4 had three No. 3 (top and bottom) bonded reinforcing steel bars. These specimens were post-tensioned with 3 – 13 mm, Grade 270 (f_{pu} = 1862 MPa) prestressing strands located at the beam centroid, in order to minimize the increase in strain caused by beam rotation. The initial stresses in the prestressing strands were 0.46 f_{pu} for M-P-Z4, and 0.41 f_{pu} for O-P-Z4. The columns were subjected to a constant axial load and a cyclic lateral load based on story drift in the test.

In the numerical models, both beams are represented by 22 elements, while both columns are represented by 9 elements as shown in Figure 4. The beam and column elements are connected through the beam – column joint element. The cross-sections of the beam and column elements are divided into 65 and 45 concrete layers respectively. The material properties used in the analysis are as follows: For the concrete, the compressive strength, tensile strength and initial stiffness are 51.0 MPa, 4.3 MPa and 34.0 GPa in specimen M-P-Z4, and 53.0 MPa, 4.4 MPa and 35.3 GPa in specimen O-P-Z4, respectively. The yield strength and elastic modulus are 422.0 MPa and 210.0 GPa for the reinforcing steel bar, and 1710.0 MPa and 200.0 GPa for the prestressing strand, respectively. For the bond stress-slip relation of bonded reinforcing steel bar, using the formula proposed by CEB [10], the bond strength is assumed, and for the bond stress-slip relation of unbonded prestressing strand, the elastic bond stiffness is 0.001 MPa / mm.

Figure 5 compares the numerical responses with the test results for the lateral load-story drift relations of these specimens. The numerical hysteresis responses adequately agree with the test results, including the difference of each specimen's behavior due to the difference in the amount of bonded reinforcing steel bars. Another comparison between the numerical responses and the test results represented by the force variation in a

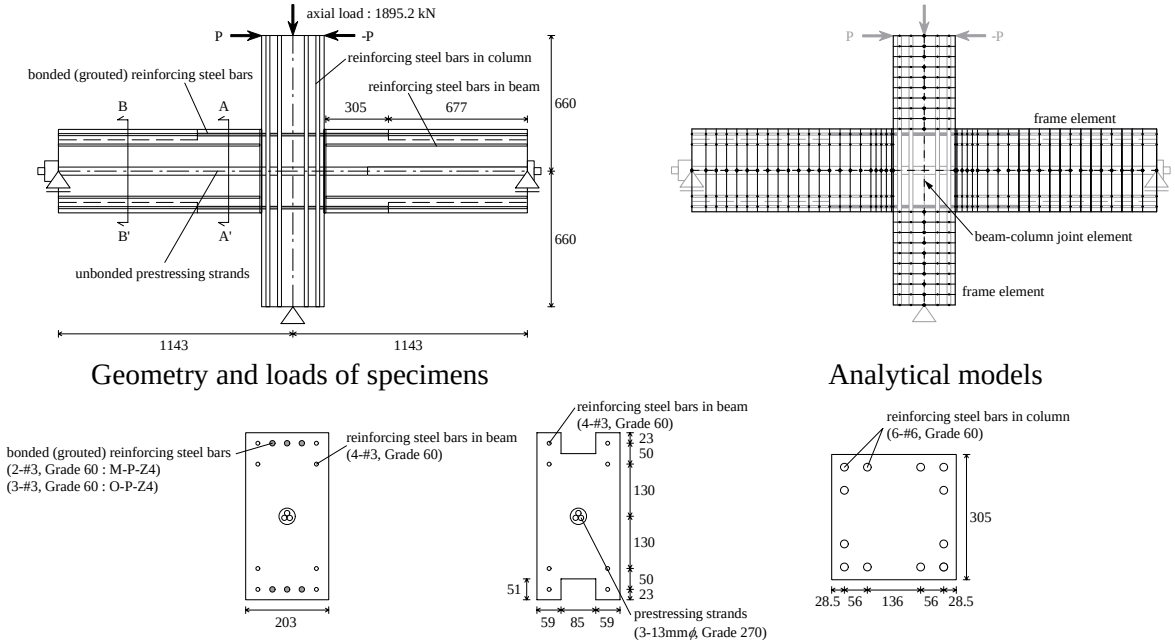

Geometry and loads of specimens | Analytical models

Beam section A-A' | Beam section B-B' | Column section

Figure 4 Geometry and loads of Stone et al. beam-to-column subassemblies [1]

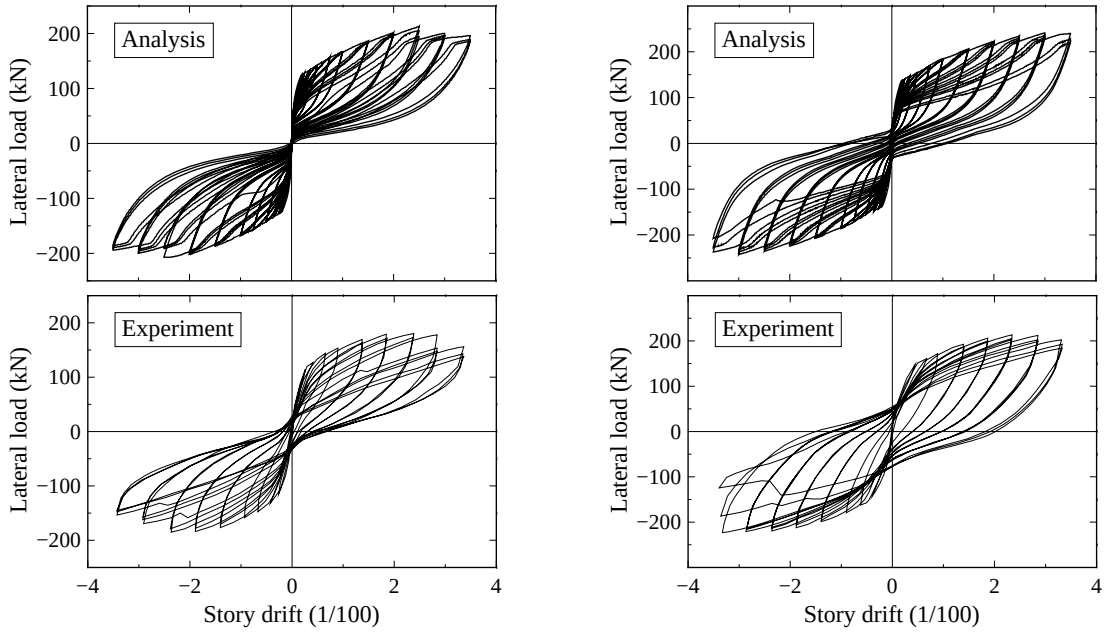

(a) Specimen M-P-Z4 (b) Specimen O-P-Z4

Figure 5 Comparison of lateral load-story drift relations

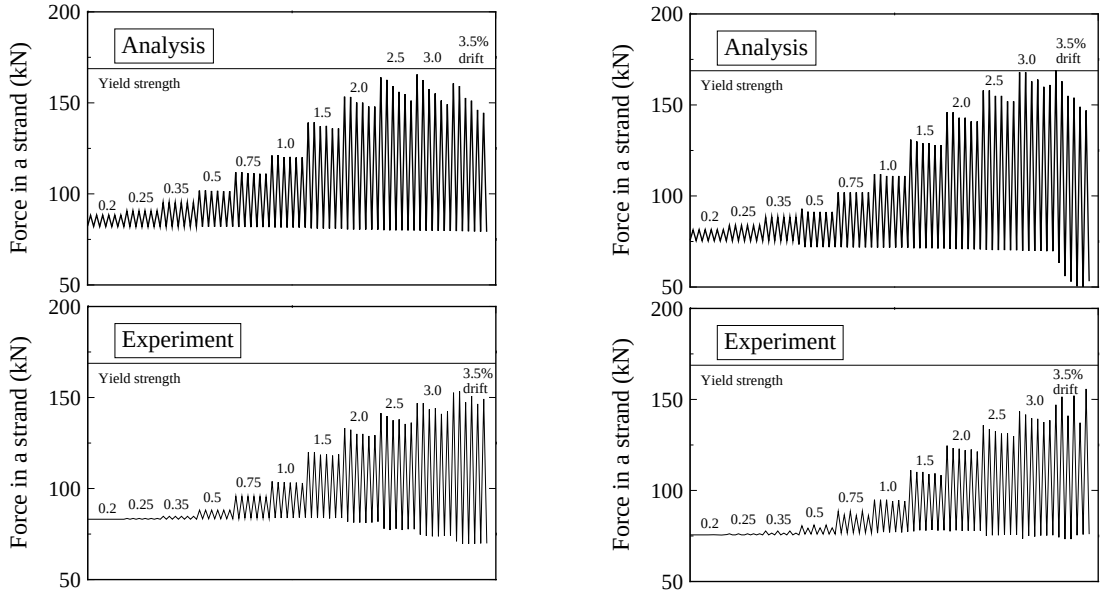

(a) Specimen M-P-Z4 (b) Specimen O-P-Z4

Figure 6 Comparison of force variation in a prestressing strand

prestressing strand and by the energy dissipated per cycle is shown in Figure 6 and 7. Overestimation of force variation and underestimation of energy dissipation are indicated. These differences most likely result from the assumption of the rigid body mode response of the joint element. However, the numerical model estimates the tendency of the test results relatively well.

4. PARAMETRIC STUDY

The most attractive features of the precast prestressed concrete frames with hybrid post-tensioned connections

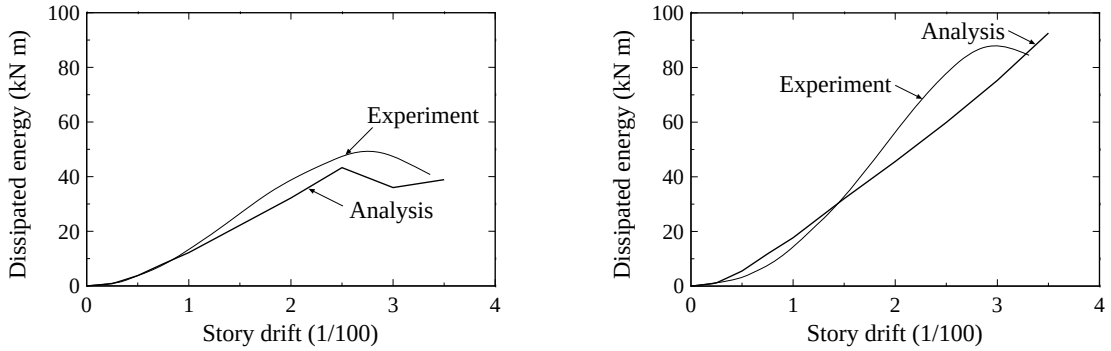

(a) Specimen M-P-Z4 (b) Specimen O-P-Z4

Figure 7 Comparison of energy dissipation

are the high restoring-force characteristics under cyclic loading and energy dissipation conditions due to the gap-opening behavior at the beam-to-column interface. The idealized moment-rotation hysteretic response developed at the beam-to-column interface of these frames is a combination of the contribution of unbonded prestressing tendons and bonded reinforcing steel bars [2]. To maintain high restoring-force characteristics, the following condition is required:

$$M_p \geq M_r \tag{4.1}$$

where M_p and M_r are the bending strengths contributed by the unbonded prestressing tendons and by the bonded reinforcing steel bars, respectively. Based on that condition, the structural performance of precast prestressed concrete frames with hybrid post-tensioned connections can be evaluated from the relation of the level of initial prestressing force P_o and the amount of bonded reinforcing steel bars A_r because M_p is related to P_o and M_r is related to A_r. To investigate the effects of variations in the connection details on the behavior of the frames, a parametric study was performed for the analytical model of the specimen M-P-Z4. The parameters of interest are P_o and A_r and seven cases were analyzed. These cases were based on the P_o / P_{oi} ratios and A_r / A_{ri} ratios where P_{oi} is the level of initial prestressing force of the specimen M-P-Z4 and A_{ri} is the amount of bonded reinforcing steel bars of the specimen M-P-Z4. The P_o / P_{oi} ratios used were 0.66, 1.33 and 2.0 in Case 1, Case 2 and Case 3. The A_r / A_{ri} ratios used were 0.5, 1.5 and 2.0 in Case 4, Case 5 and Case 6. In Case 7, both the P_o / P_{oi} ratio and the A_r / A_{ri} ratio used were 2.0. These parameters were determined by the variation of the number of unbonded prestressing strands and of bonded reinforcing steel bars arranged in specimen M-P-Z4.

Figure 8 shows the comparison of energy dissipation per cycle in each case with the numerical response of specimen M-P-Z4. With regard to the effect of the level of initial prestressing force, the dissipated energies of Case 1, Case 2 and Case 3 are approximately the same level over the entire range. The minor differences noted between these cases may be attributed to the energy dissipation of concrete in compression under each level of initial prestressing force. In Case 4, Case 5 and Case 6, the dissipated energies are different depending on the amount of bonded reinforcing steel bars. At the same story drift, the energy increased with the increase of the amount of bonded reinforcing steel bars, and, because the story drift was incremented, the difference of the

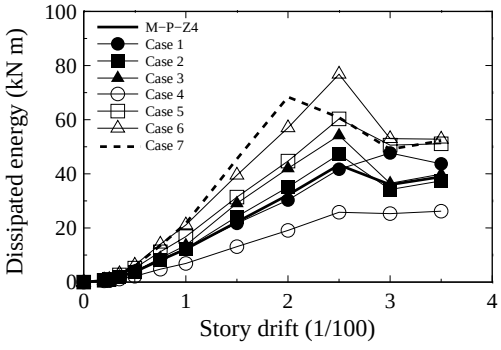

Figure 8 Comparison of energy dissipation

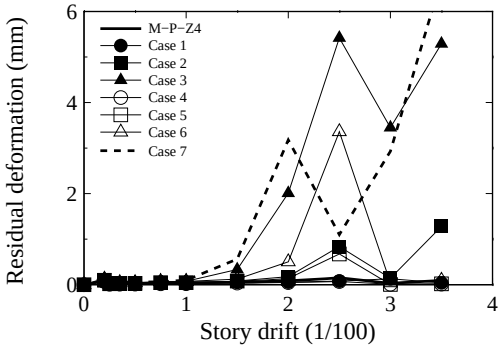

Figure 9 Comparison of residual deformation

energy in these cases is larger. These results indicate that energy dissipation of these subassemblies can be estimated from the amount of bonded reinforcing steel bars.

Figure 9 shows the comparison of residual deformation per cycle of each case. The residual deformation is observed clearly in Case 2, Case 3, Case 5, Case 6 and Case 7. The results of Case 2, Case 3 and Case 7 with increased levels of initial prestressing force indicate the effect of residual strain of concrete in compression. In Case 5 and Case 6, it appears that the ratio of the level of initial prestressing force to the amount of bonded reinforcing steel bars affects the results, as is shown in Eqn. 4.1.

5. CONCLUSIONS

The structural performance of precast prestressed concrete frames connected by hybrid post-tensioned connections under cyclic loading were analytically investigated. The analytical models used in this paper are based on the finite element method. One is a frame element, and the other is a beam-column joint element. The models include bond slip effects between reinforcing steel bars and concrete and between bonded or unbonded prestressing tendons and concrete. The comparison of numerical and experimental results has demonstrated the good performance of the analytical models in terms of the hysteretic behavior of lateral load-story drift relations, force variation in a prestressing strand, and energy dissipation. The results of the parametric study for the subassemblies indicate that energy dissipation can be estimated from the amount of bonded reinforcing steel bars, and the self-centering capability can be evaluated from the ratio of the level of initial prestressing force to the amount of bonded reinforcing steel bars.

REFERENCES

1. Stone, W. C., Cheok, G. S. and Stanton, J. F. (1995). Performance of hybrid moment-resisting precast beam-column concrete connections subjected to cyclic loading. *ACI Structural Journal* **92:2**, 229-249.
2. Sugata, M. and Nakatsuka, T. (2004). Experimental study for load-deflection characteristics of precast prestressed flexural members with unbonded tendon and mild steel. *Journal of Structural and Construction Engineering* **584**, 153-159. (In Japanese)
3. Koshikawa, T., Saito, T., Ueda, M. and Kikuchi, M. (2004). Hysteretic behavior analysis of PCaPC beam-columns assembled by prestressing steel with bond-slip. *Proceedings of the Japan Concrete Institute* **26:2**, 37-42. (In Japanese)
4. Saito, T., Koshikawa, T., Ueda, M. and Kikuchi, M. (2005). Hysteretic behavior analysis of RC plane frames considering bond-slip in beam-column joint. *Proceedings of the Japan Concrete Institute* **27:2**, 73-78. (In Japanese)
5. Kabaila, A., Sanez, L. P., Tulin, L. G. and Gerstle, K. H. (1964). Discussion of 'Equation for the stress-strain curve of concrete, by Desayi, P. and Krishnan, S.'. *ACI Journal, Proceedings* **61:9**, 1227-1239.
6. Nakamura, H., and Higai, T. (1999). Compressive fracture energy and fracture zone length of concrete. *Seminar on Post-Peak Behavior of RC Structures Subjected to Seismic Loads, Japan Concrete Institute* **2**, 259-272.
7. Karsan, I. D. and Jirsa, J. O. (1969). Behavior of concrete under compressive loadings. *Journal of the Structural Division, ASCE* **95:ST12**, 2543-2563.
8. Ueda, M. and Dobashi, Y. (1985). Nonlinear bond slip analysis of axially loaded reinforced concrete prismatic members. *Proceedings of the Japan Society of Civil Engineers* **360:V-3**, 71-80. (In Japanese)
9. Morita, S. and Kaku, T. (1975). Bond-slip relationship under repeated loading. *Transactions of the Architectural Institute of Japan* **229**, 15-24. (In Japanese)
10. Comite Euro-International du Beton. (1990). CEB-FIP Model Code 1990, First Draft, CEB.